JACS
JOURNAL OF THE AMERICAN CHEMICAL SOCIETY
Article
pubs.acs.org/JACS

Entropic Origin of Cobalt–Carbon Bond Cleavage Catalysis in Adenosylcobalamin-Dependent Ethanolamine Ammonia-Lyase

Miao Wang‡ and Kurt Warncke*

Department of Physics, Emory University, Atlanta, Georgia 30322, United States

Supporting Information

ABSTRACT: Adenosylcobalamin-dependent enzymes accelerate the cleavage of the cobalt–carbon (Co–C) bond of the bound coenzyme by >10^{10}-fold. The cleavage-generated 5′-deoxyadenosyl radical initiates the catalytic cycle by abstracting a hydrogen atom from substrate. Kinetic coupling of the Co–C bond cleavage and hydrogen-atom-transfer steps at ambient temperatures has interfered with past experimental attempts to directly address the factors that govern Co–C bond cleavage catalysis. Here, we use time-resolved, full-spectrum electron paramagnetic resonance spectroscopy, with temperature-step reaction initiation, starting from the enzyme–coenzyme–substrate ternary complex and ^{2}H-labeled substrate, to study radical pair generation in ethanolamine ammonia-lyase from *Salmonella typhimurium* at 234–248 K in a dimethylsulfoxide/water cryosolvent system. The monoexponential kinetics of formation of the ^{2}H- and ^{1}H-substituted substrate radicals are the same, indicating that Co–C bond cleavage rate-limits radical pair formation. Analysis of the kinetics by using a linear, three-state model allows extraction of the microscopic rate constant for Co–C bond cleavage. Eyring analysis reveals that the activation enthalpy for Co–C bond cleavage is 32 ± 1 kcal/mol, which is the same as for the cleavage reaction in solution. The origin of Co–C bond cleavage catalysis in the enzyme is, therefore, the large, favorable activation entropy of 61 ± 6 cal/(mol·K) (relative to 7 ± 1 cal/(mol·K) in solution). This represents a paradigm shift from traditional, enthalpy-based mechanisms that have been proposed for Co–C bond-breaking in B_{12} enzymes. The catalysis is proposed to arise from an increase in protein configurational entropy along the reaction coordinate.

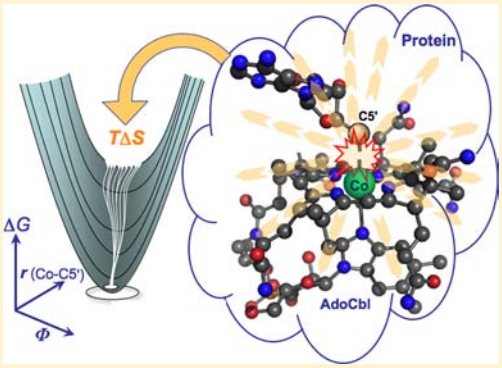

INTRODUCTION

The cobalt–carbon bond in the adenosylcobalamin (AdoCbl; coenzyme B_{12}) cofactor in B_{12} enzymes is cleaved homolytically to generate the 5′-deoxyadenosyl radical.[1−3] This highly reactive species abstracts hydrogen from substrates to initiate the core rearrangement reaction. The reaction sequence that leads to formation of the cob(II)alamin–substrate radical pair is depicted in Figure 1. B_{12} enzymes elevate the rate of homolytic cleavage of the coenzyme's Co–C bond to a biologically commensurate value of >10^{1} s^{-1},[1−3] relative to the rate of approximately 10^{-9} s^{-1} in solution.[4] Elucidation of the energetics and molecular mechanism of this remarkable >10^{10}-fold rate acceleration has been the focus of theoretical and experimental efforts for four decades.[1−3,5] However, the kinetic coupling of Co–C bond cleavage to the subsequent hydrogen-atom-transfer reaction has interfered with a clean experimental assessment of Co–C bond cleavage catalysis. The kinetic coupling was revealed in room-temperature stopped-flow experiments, performed on the enzymes methylmalonyl-CoA mutase (MCM),[6] glutamate mutase (GM),[7,8] ribonucleotide triphosphate reductase (RTPR),[9] and ethanolamine ammonia-lyase (EAL).[10] The time dependence of the visible absorption change from the intact adenosylcob(III)alamin (λ_{max} ≈ 525 nm) to the cleaved cob(II)alamin (λ_{max} ≈ 470 nm) displayed substrate ^{1}H/^{2}H hydrogen isotope effects of 2 to >20.[6,7,9,10] A related obstacle to characterizing the reaction has been the inability to detect and distinguish the proposed cob(II)alamin–5′-deoxyadenosyl radical pair intermediate by using optical methods. Thus, the stopped-flow kinetics have been provisionally treated by using a model for the radical pair separation, in which the Co–C bond cleavage and hydrogen-transfer steps are combined in a single formal step.[6,7,9,10] The existence of the 5′-deoxadenosyl radical species as a discrete chemical intermediate has also been questioned.[11]

Proposed mechanisms for Co–C bond cleavage catalysis in AdoCbl-dependent enzymes have been based on enthalpic factors and have included protein-promoted *trans*- and *cis*-axial ligand effects (both electronic and steric), corrin ring flexure, and distortions of the Co–C bond, which represent ground-state destabilization mechanisms[12,13] (for reviews, see refs 5 and 14). In EAL, Co–C bond photolysis and UV–visible spectroscopic studies show that AdoCbl is not significantly distorted in the enzyme–coenzyme–substrate ternary complex[15,16] and that substrate binding does not switch the protein to a structural state that promptly stabilizes radical pair formation.[16] Detailed microscopic mechanisms that involve the development of favorable binding energy between the

Received: May 8, 2013
Published: September 12, 2013

   dx.doi.org/10.1021/ja404467d | J. Am. Chem. Soc. 2013, 135, 15077–15084

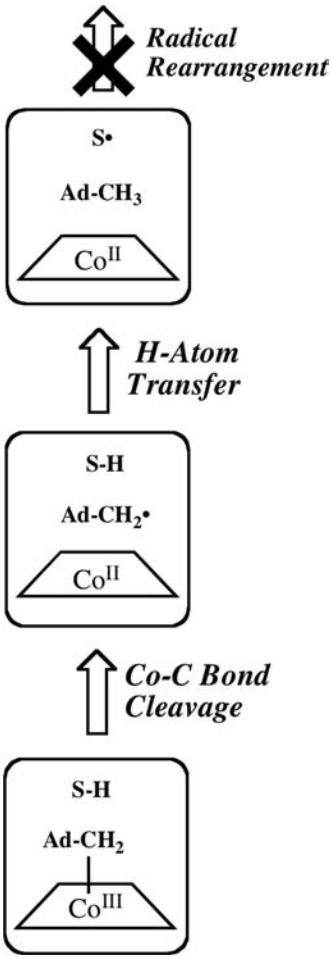

Figure 1. Minimal mechanism for formation of the Co(II)−substrate radical pair from the ternary complex in AdoCbl-dependent ethanolamine ammonia-lyase.[18,30] The forward direction of reaction through the Co−C bond cleavage and hydrogen-atom-transfer steps is indicated by arrows. For substrate (*S*)-2-aminopropanol, the steps are reversible, and decay of the substrate radical through the product radical is 10^2-fold slower than equilibration of the first two steps.[18,30] Thus, radical rearrangement is not significant on the time scale of the experiments reported here,[25] as indicted by the "X". Substrate-derived species are designated S-H (bound substrate) and S$^\bullet$ (substrate radical). The 5′-deoxyadenosyl β-axial ligand is represented as Ad-CH_2− in the intact coenzyme, and as Ad-$CH_2^\bullet$ (5′-deoxyadenosyl radical) or Ad-CH_3 (5′-deoxyadenosine) following Co−C bond cleavage. The cobalt ion and its formal oxidation states are depicted, but the corrin ring and dimethylbenzimidazole α-axial ligand of the coenzyme[61,62] are not shown, for clarity.

protein and the 5′-deoxyadenosyl radical, which represent transition-state stabilization mechanisms, have also been proposed, based on theory and modeling.[17−20] Spectroscopic studies, including UV−visible absorption, magnetic circular dichroism (MCD), and resonance Raman, have shown that AdoCbl is not significantly distorted in the MCM holoenzyme, or in the presence of substrate analogues, relative to solution.[21] The structure of the cleavage product, cob(II)alamin, is also not significantly influenced by the protein.[22] An absence of significant ground-state Co−C bond activation by the enzyme was also concluded from infrared[23] and picosecond optical[24] spectroscopic studies. The factors that govern enzymic Co−C bond cleavage catalysis have therefore remained elusive.

Time-resolved, full-spectrum electron paramagnetic resonance (EPR) spectroscopy in a fluid, low-temperature 41% v/v (14% mol/mol) dimethylsulfoxide (DMSO)/water cryosolvent system was developed to address the mechanism of Co−C bond cleavage and cob(II)alamin−substrate radical pair formation in EAL from *Salmonella typhimurium*, by directly detecting the time evolution of the paramagnetic radical pair species.[25] EAL [EC 4.3.1.7; cobalamin (vitamin B_{12})-dependent enzyme superfamily;[26,27] X-ray crystallographic structure of *Escherichia coli* EAL;[13] structural model of *S. typhimurium* EAL[28]] converts aminoethanol and (*R*)- and (*S*)-2-aminopropanols to the corresponding aldehydes and ammonia.[29,30] The kinetically arrested EAL−adenosylcobalamin−substrate ternary complex was prepared by mixing holoenzyme with (*S*)-2-aminopropanol substrate in the cryosolvent at 230 K (lifetime, 4 h). The reaction is subsequently initiated by temperature step (*T*-step) to 234−248 K.[25] In this system, the reaction lifetime/deadtime ratio is increased by $>10^2$, relative to room-temperature mixing experiments, and the reaction lifetimes (5−60 min) are significantly slower than the EPR spectrum acquisition time (24 s, minimum). The mono-exponential rise of the Co(II)−substrate radical pair intermediate yielded the measured parameters, k_{obs} (observed rate constant) and ν [normalized concentration of Co(II)−substrate radical pair]. The results were interpreted in terms of a linear two-step, three-state mechanism, which included the ternary complex, the Co(II)−substrate radical pair, and the explicit incorporation of the Co(II)−5′-deoxyadenosyl radical pair intermediate.[25] The absence of detectable paramagnetic species, other than the Co(II)−substrate radical pair, showed that the Co(II)−5′-deoxyadenosyl radical pair lies >3.3 kcal/mol higher in free energy than the Co(II)−substrate radical pair. The temperature dependence of the equilibrium between the ternary complex and the Co(II)−substrate radical pair state revealed that EAL biases the radical pair separation process in the forward direction by −2.6 ± 1.2 kcal/mol at 298 K.

Here, we report that k_{obs} for formation of the Co(II)−substrate radical pair in EAL in the cryosolvent system with 1-$^2H_2$-(*S*)-aminopropanol (^{2}H-substrate) is the same, to within the measurement uncertainty, as for natural abundance ^{1}H-substrate. This indicates that Co−C bond cleavage is the rate-determining step for radical pair separation in EAL at low temperature (234−248 K). The negligible concentration of the Co(II)-5′-deoxyadenosyl radical pair intermediate (<0.1% of the total active sites) simplifies the kinetic description of the reaction in terms of the linear three-state mechanism and allows the determination of the first-order rate constant for Co−C bond cleavage (k_{12}). The temperature dependence of k_{12} reveals that Co−C bond cleavage catalysis (relative to solution) in EAL is driven by a large, favorable activation entropy. This represents a paradigm shift for mechanistic proposals for the Co−C bond cleavage process in B_{12} enzymes. A model for protein configurational entropy contributions to enzyme catalysis is proposed.

MATERIALS AND METHODS

Materials. All chemicals were obtained from commercial sources (Sigma-Aldrich or Fisher) and were used without further purification. Enzyme was purified from the *Escherichia coli* overexpression strain incorporating the cloned *S. typhimurium* EAL coding sequences[31] essentially as described,[32] with the exception that the enzyme was dialyzed against a final buffer containing 100 mM HEPES (pH 7.5), 10 mM potassium chloride, 5 mM dithiothreitol, and 10% glycerol.

dx.doi.org/10.1021/ja404467d | J. Am. Chem. Soc. 2013, 135, 15077−15084

Synthesis of [1,1-$^2H_2$]-(*S*)-2-Aminopropanol. [1,1-$^2H_2$]-(*S*)-2-Aminopropanol was synthesized from L-alanine methyl ester, as described.[10] The purity of the product was verified by mass spectrometry and ^1H NMR.[33]

Preparation of the Ternary Complex in the Cryosolvent System. The preparation of EAL in DMSO/water cryosolvent has been described in detail.[25] Briefly, a 1.5-fold excess of AdoCbl relative to EAL active sites was introduced into buffered 10 mM potassium cacodylate (pH = 7.1 at 298 K; pH = 7.5 ± 0.2 at 234−248 K), and DMSO was added incrementally in four steps with descending temperature to a final proportion of 41% (v/v) at 230 K. The 41% (v/v) DMSO/water solution is fluid at 234−248 K. Natural abundance or 1,1-$^2H_2$-(*S*)-2-aminopropanol in 41% (v/v) DMSO/water was introduced at 230 K with mixing to form the ternary complex. All the procedures were performed under a dim red safe light, because the Co−C bond is sensitive to photolysis, and the long-wavelength visible absorbance maximum of the cofactor is 523 nm.[16]

Time-Resolved EPR Spectroscopy. X-band continuous wave (CW)-EPR experiments were carried out on a Bruker ELEXSYS E500 EPR spectrometer with an ER 4123SHQE X-band cavity resonator and a Bruker ER 4131VT temperature control system. All of the temperature readings in the EPR experiments were measured by using an Oxford Instruments ITC503 temperature controller with a calibrated model 19180 4-wire RTD probe. The total temperature error of the measurements was estimated to be ±0.4 K. The decrease in cavity quality factor caused by the lossy liquid samples was mitigated by using 2 mm outer diameter capillary sample tubes (712-SQ-250M; Wilmad-Lab Glass, Buena, NJ). The reaction of the holoenzyme−substrate mixture was triggered by a *T*-step (set point change) from 230 K to the desired higher temperature (234−248 K). The dead time of the system, including the temperature increase, equilibration, and microwave bridge balancing at the high-temperature set point, was ≤30 s.

Equilibrium Perturbation Experiments. A sample (300 μL) was prepared in a 4 mm outer diameter EPR tube with 100-fold excess of substrate compared to EAL active sites. The sample was initially adjusted to the incubation temperature, T_{inc}, in the ER 4123SHQE X-band cavity resonator and incubated to achieve a constant amplitude of the Co(II)−substrate radical pair EPR signal. The temperature of the sample was then quickly decreased to 120 K, and the EPR spectrum was acquired to obtain the EPR signal amplitude for the substrate radical [peak-to-trough amplitude, $A_{pt}(t = \infty, T = T_{inc})$]. After finishing all desired incubation temperatures, the sample temperature was raised stepwise to 273 K to form the Co(II)−substrate radical pair in 100% of the functional EAL active sites (ν = 1.0 at 273 K).[34] The fraction of EAL active sites occupied by the Co(II)−substrate radical pair, ν_i, was computed for each incubation temperature, T_i, by normalizing $A_{pt}(\infty,T_{inc})$ to the $A_{pt}(\infty,273\ K)$.

Curve fitting was performed by using the program OriginPro 7.5 (OriginLab Corp., Northampton, MA) with the least-squares fitting method.

Kinetic Model. The time dependence of the rise of the Co(II)−substrate radical pair EPR signal, following *T*-step of the ternary complex, is analyzed by using the three-state mechanism shown in Scheme 1,[35] where the states A_1, A_2, and A_3 represent the ternary complex, the Co(II)−5′-deoxyadenosyl radical pair, and the Co(II)−substrate radical pair, respectively. Co−C bond cleavage and reformation is represented by microscopic first-order rate constants, k_{12} and k_{21}, respectively, and equilibrium constant, $K_{12} = k_{12}/k_{21}$. The hydrogen-atom-transfer steps are represented by microscopic first-order rate constants, k_{23} and k_{32}, and equilibrium constant, $K_{23} = k_{23}/k_{32}$. We have previously shown that the A_2 intermediate is not detectable by using EPR, with a limit of $[A_2]_t/[A_3]_t < 10^{-3}$, where the *t* subscript indicates any time during the rise of A_3, or after equilibrium is reached.[25] This situation corresponds to the condition $k_{12}, k_{32} \ll k_{21}, k_{23}$, which leads to simplified expressions for the observed first-order rate constant for the EPR-detected growth of A_3, and for the normalized equilibrium amplitude of A_3 ($\nu = [A_3]_\infty/[A_1]_0$), in terms of the microscopic rate constants, as follows:[25]

Scheme 1

$$A_1 \underset{k_{21}}{\overset{k_{12}}{\rightleftharpoons}} A_2 \underset{k_{32}}{\overset{k_{23}}{\rightleftharpoons}} A_3$$

$$k_{obs} = \frac{k_{12}k_{23} + k_{21}k_{32}}{k_{21} + k_{23}} \quad (1)$$

$$\nu = \frac{k_{12}k_{23}}{k_{12}k_{23} + k_{21}k_{32}} \quad (2)$$

Multiplication of eq 1 by eq 2 and rearrangement leads to the following expression for the first-order rate constant for Co−C bond cleavage:

$$k_{12} = k_{obs}\nu\left(1 + \frac{k_{21}}{k_{23}}\right) \quad (3)$$

The coupling term, $1 + k_{21}/k_{23}$, incorporates the ratio of the reverse and forward rate constants for decay from the A_2 state. Equation 3 shows that, if $k_{21}/k_{23} \ll 1$, then k_{12} can be determined from measured parameters. The standard deviations for products and quotients of measured parameters were calculated by established procedures.[36] The standard deviation of the mean (σ_{mean}) corresponding to mean isotope effects was evaluated from the expression for the normalized geometric sum of the *n* individual variances (σ_i^2) as follows: $\sigma_{mean}^2 = (1/n^2)\sum_{i=1}^{n}\sigma_i^2$.[36]

The temperature dependence of the first-order rate constant, $k(T)$, is given by the Eyring expression,[35] as follows:

$$\ln\frac{k(T)}{T} = \ln\frac{k_B}{h} + \frac{\Delta S^{\ddagger}}{R} - \frac{\Delta H^{\ddagger}}{RT} \quad (4)$$

where $\Delta H^{\ddagger}$ and $\Delta S^{\ddagger}$ are the activation enthalpy and activation entropy, respectively, for Co−C bond cleavage, k_B is Boltzmann's constant, and *h* is Planck's constant. The parameters $\Delta H^{\ddagger}$ and $\Delta S^{\ddagger}$ are determined by a linear fitting of the plot of $\ln k(T)/T$ versus $1/T$. The activation free energy, $\Delta G^{\ddagger}$, is calculated by using the expression $\Delta G^{\ddagger} = \Delta H^{\ddagger} - T\Delta S^{\ddagger}$.

RESULTS

Figure 2 shows the time dependence of the rise of the ^2H-substrate radical EPR spectrum at 246 K, following *T*-step from 230 K. The steady-state equilibrium EPR spectra of the Co(II)−substrate radical pair,[37] formed by using either ^2H- or ^1H-substrate, are presented in the Supporting Information (Figure S1). As shown by the plot and fit of the peak-to-trough EPR amplitude (A_{pt}) of the substrate radical as a function of time in Figure 3, the single-exponential growth leads to a stable amplitude at long times, which corresponds to ν = 0.4−0.6 for *T* = 236−246 K. Analysis of the individual EPR spectra collected for ^2H-substrate, both during the rise of the substrate radical and following equilibration, does not provide evidence of paramagnetic species other than the Co(II)−substrate radical pair, above the substrate radical signal-to-noise level of 10^3, as previously described for reaction of the ^1H-substrate.[25] Therefore, the proportion of the intermediate Co(II)−5′-deoxyadenosyl radical pair is $<10^{-3}$, relative to the substrate radical. The values of k_{obs} and ν, collected over the temperature range of 234−246 K for the ^2H-substrate, and values determined previously for reaction with the ^1H-substrate,[25,33] are presented in Table 1.

Table 1 shows the substrate isotope effects on k_{obs} and ν at each temperature. The average of the substrate $^1H/^2H$ isotope effect on k_{obs} over 234−246 K is 0.93 ± 0.08, which is unity to

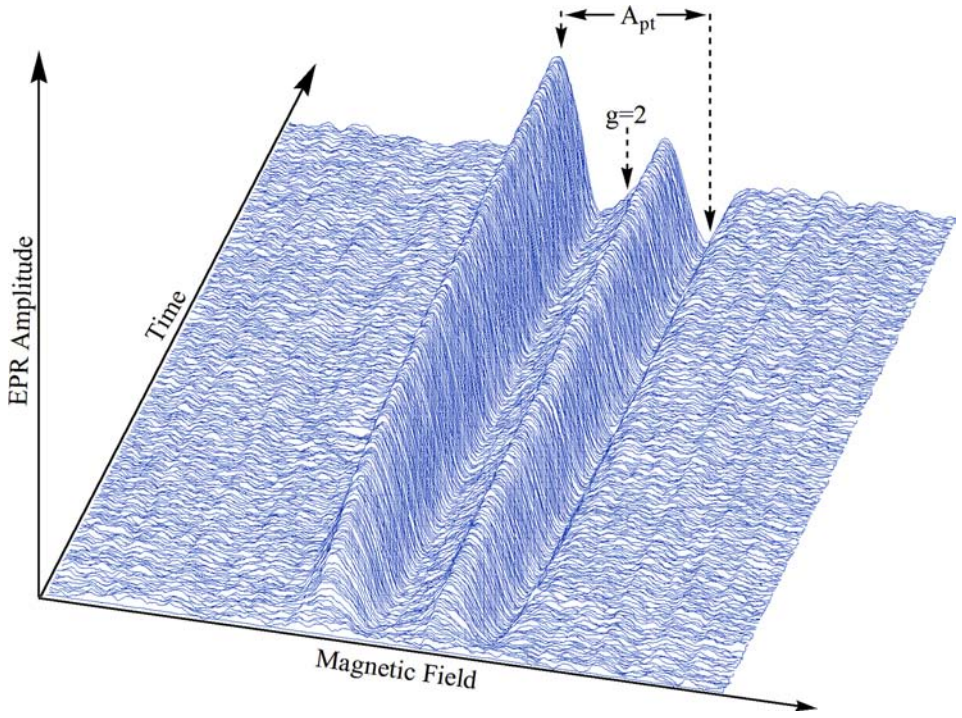

Figure 2. Time-resolved, full-spectrum EPR spectroscopy of the substrate radical formed from ^{2}H-labeled substrate in the cryosolvent system at T = 246 K, following T-step initiation of reaction. The free electron resonance position at g = 2.0 is shown by the arrow. The full extents of the magnetic field sweep and time course are 560 G and 6.43 × 10^3 s, respectively. The first peak and second trough, which are used to determine A_{pt}, are positioned at 3284 and 3415 G, respectively. The concentrations of EAL active sites and substrate are 150 μM and 15 mM, respectively. EPR conditions: microwave frequency, 9.365 GHz; microwave power, 10 dB (20 mW); magnetic field modulation, 12 G; modulation frequency, 100 kHz; interscan interval, 15 s; scan rate, 53 G s^{-1}; time constant, 164 μs. The t = 0 spectrum (baseline) has been subtracted from each spectrum.

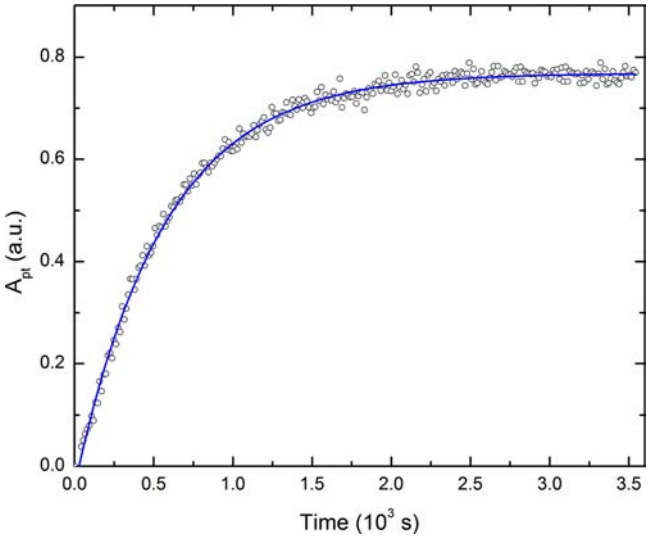

Figure 3. Time dependence of the EPR amplitude of the substrate radical formed from ^{2}H-labeled subtstrate in EAL in the cryosolvent system at T = 246 K, following T-step initiation of reaction. The data are truncated at 3.90 × 10^3 s, relative to the full time scale of 6.43 × 10^3 s presented in Figure 2. The experimental data points are overlaid with the best-fit exponential growth function (solid curve; k_{obs}= 1.82 × 10^{-3} s^{-1}). EPR conditions are as described in the legend to Figure 2.

within one standard deviation. Plots of ln k_{obs} versus $1/T$ for the ^{2}H- and ^{1}H-substrates also give the same linear fit parameters, to within one standard deviation (Figures S2 and S3). The absence of a significant substrate hydrogen isotope effect on k_{obs} indicates that hydrogen-atom transfer is not rate-determining for the formation of the Co(II)−substrate radical pair over the temperature range of 234−246 K. In contrast, the substrate ^{1}H/^{2}H isotope effect on the rate of formation of cob(II)alamin following mixing EAL holoenzyme with substrate in stopped-flow studies at room temperature is 3.1 ± 0.3.[10]

The average of the substrate ^{1}H/^{2}H isotope effect on ν over 238−246 K is 1.07 ± 0.07, which is also unity to within one standard deviation. This equilibrium isotope effect depends on differences in bonding [as characterized by changes in vibrational modes and frequencies,[38] or the related bond dissociation energies (BDE)] at the sites of ^{2}H substitution, between the A_1 and A_3 states. The value of near unity is consistent with a relatively small overall change in the C−H BDE values, as expected for the transformation of two α-hydroxy C−H (sp^3 carbon) bonds in the substrate in A_1 to an alkyl C5′−H bond (sp^3 carbon) and a C1−H bond (α-hydroxy radical center, sp^2 carbon) in A_3, within the uncertainties of the in situ effects of hydrogen bonding at the hydroxyl oxygen- and geometry-dependent resonance stabilization.[8,39−43]

■ DISCUSSION

Rate Constant for Co−C Bond Cleavage. The absence of a significant substrate hydrogen isotope effect on the observed rate of formation of the Co(II)−substrate radical pair indicates that the Co−C bond cleavage step is not kinetically coupled to the hydrogen transfer at low temperatures of 234−246 K. Therefore, we propose that the Co−C bond cleavage step is rate-determining for radical pair formation in the low-temperature range. In terms of the three-state mechanism (Scheme 1), this implies that the free energy of the transition

dx.doi.org/10.1021/ja404467d | J. Am. Chem. Soc. 2013, 135, 15077−15084

Table 1. Values of the Observed Rate Constants for Co(II)−Substrate Radical Pair Formation and the Normalized Population of the Co(II)−Substrate Radical Pair for ^{1}H- and ^{2}H-Substrate, and Their Ratios, at Different Absolute Temperatures[a]

T (K)	$k_{obs,H}$ ($\times 10^3$ s^{-1})	$k_{obs,D}$ ($\times 10^3$ s^{-1})	$k_{obs,H}/k_{obs,D}$	ν_H	ν_D	ν_H/ν_D
234	0.29 ± 0.06	0.28 ± 0.08	1.0 ± 0.3	–	–	–
236	0.39 ± 0.04	0.51 ± 0.01	0.8 ± 0.1	–	–	–
238	0.58 ± 0.08	0.70 ± 0.1	0.8 ± 0.2	0.39 ± 0.07[b]	0.357 ± 0.004	1.09 ± 0.19
240	1.1 ± 0.07	1.0 ± 0.2	1.1 ± 0.2	0.44 ± 0.06	0.391 ± 0.001	1.13 ± 0.15
242	1.5 ± 0.2	1.9 ± 0.1	0.8 ± 0.1	0.48 ± 0.06	0.46 ± 0.03	1.05 ± 0.14
244	2.5 ± 0.5	3.1 ± 0.2	0.8 ± 0.1	0.53 ± 0.05	0.50 ± 0.05	1.06 ± 0.14
246	4.4 ± 0.3	3.8 ± 0.3	1.2 ± 0.1	0.56 ± 0.05	0.55 ± 0.05	1.02 ± 0.13
248	6.2 ± 0.9	–	–	0.61 ± 0.04	–	–

[a]Values represent the average of at least three separate experiments, with the exception of the ν_D parameters (two separate experiments), and the corresponding standard deviations. Values of $k_{obs,H}$ and ν_H were reported previously[25,33] and are included to illustrate determination of the ratio parameters and corresponding standard deviations. [b]Mean and standard deviation for one measured value and two values obtained by linear extrapolation of two separate measured ν_H dependences on temperature over 240−248 K.

state for Co−C bond cleavage is significantly higher than the transition state for hydrogen transfer and, therefore, that $k_{21} \ll k_{23}$. Thus, eq 3 simplifies to the following form, which allows the determination of k_{12} from measured parameters:

$$k_{12} = k_{obs}\nu \quad (5)$$

Values of $k_{12,H}$ and $k_{12,D}$ and their ratios at the different temperatures are collected in the Supporting Information (Table S1). The hydrogen isotope effect on k_{12}, which corresponds to the ratio of $k_{12,H}/k_{12,D}$ calculated by using eq 5 and the isotope effect for k_{obs} and ν in Table 1, is 1.00 ± 0.10. Therefore, the hydrogen isotope effect is unity, to within one standard deviation. This supports the assumptions that lead to eq 5. The isotope independence of the reaction implies the existence of the Co(II)−5′-deoxyadenosyl radical pair as a discrete intermediate in EAL. This is because concerted reaction of A_1 to form A_3 is predicted to involve a hydrogen isotope effect. A transient Co(II)−5′-deoxyadenosyl radical pair has also been evidenced in the deoxyguanosine triphosphate (dGTP)-activated RTPR by hydrogen isotope studies that show epimerization of the C5′ center.[44]

Activation Parameters for Co−C Bond Cleavage in EAL. Figure 4 shows the Eyring plot for $k_{12,H}$ and the excellent fit achieved by using the linear relation. Extrapolation of the linear fit in Figure 4 to 298 K yields a value of $k_{12,H}$ = 300 s^{-1}.

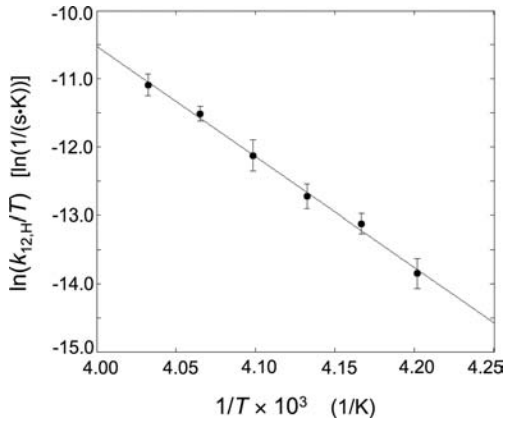

Figure 4. Eyring plot of the first-order rate constant for Co−C bond cleavage for ^{1}H-substrate. The error bars represent the standard deviation obtained by combining three separate measurements at each temperature. Best linear fit (solid line) parameters: slope = -1.62×10^4, ordinate intercept = 5.43×10^1, R^2 = 0.996.

This value is 4-fold greater than the rate of 74 s^{-1} for cob(II)alamin formation measured by stopped-flow/visible absorbance spectroscopy at room temperature.[10] The relatively high extrapolated rate is consistent with a change in the rate-determining step for radical pair separation, from Co−C bond cleavage at low (234−248 K) temperatures to the hydrogen-transfer step at ambient temperatures. The slope and intercept of the Eyring plot lead to values for the activation enthalpy and activation entropy of Co−C bond cleavage of $\Delta H^{\ddagger}_{12}$ = 32 ± 1 kcal/mol and $\Delta S^{\ddagger}_{12}$ = 61 ± 6 cal/(mol·K), respectively. Thus, the free energy of activation varies from $\Delta G^{\ddagger}_{12}$ = 18 ± 2 kcal/mol at 238 K to 17 ± 2 kcal/mol at 248 K. The favorable contribution of the term $-T\Delta S^{\ddagger}_{12}$ to $\Delta G^{\ddagger}_{12}$ becomes smaller as the temperature is lowered. This leads to the observed rate limitation by Co−C bond cleavage at low temperature.

Entropic Origin of Cobalt−Carbon Bond Cleavage Catalysis in EAL. Figure 5 shows a schematic diagram of the contributions of the activation parameters to the uncatalyzed Co−C bond cleavage reaction in aqueous solution ($\Delta H^{\ddagger}_S$, $T\Delta S^{\ddagger}_S$, and $\Delta G^{\ddagger}_S$) and in EAL ($\Delta H^{\ddagger}_{12}$, $T\Delta S^{\ddagger}_{12}$, and $\Delta G^{\ddagger}_{12}$) at T = 298 K. In aqueous solution, the large value of $\Delta H^{\ddagger}_S$ (31.8 ± 0.7 kcal/mol) dominates $\Delta G^{\ddagger}_S$ (30 ± 1 kcal/mol), because of the relatively small positive value of $\Delta S^{\ddagger}_S$ (6.8 ± 1.0 cal/(mol·K); $T\Delta S^{\ddagger}_S$ = 2.0 ± 0.3 kcal/mol).[45] The values of $\Delta H^{\ddagger}_{12}$ and $\Delta H^{\ddagger}_S$ are the same, to within the measurement uncertainties. Therefore, as depicted in Figure 5A, catalysis of Co−C bond cleavage in EAL, relative to solution, originates from the large, favorable activation entropy. This represents a paradigm shift from previous enthalpy-based proposals for enzymic Co−C bond cleavage catalysis.[5,14,17,18] As depicted in Figure 5B, a significant fraction of the increased entropy at the transition state for Co−C bond cleavage is maintained in the Co(II)−substrate radical pair state.[25] Thus, the increase in entropy also makes a significant contribution to the thermodynamic driving force for radical pair separation.

Effective activation parameters for Co(II)−radical pair formation, under conditions of kinetic coupling[6,7,9,10] of the Co−C bond cleavage and a hydrogen-transfer step, have been reported for RTPR (278−298 K)[46] and MCM (298−313 K).[47] In these rapid-mixing, pre-steady-state kinetic studies, the mechanism used to analyze the results involved a first step, representing the diffusive encounter of enzyme and substrate, and a second step, representing a combination of the Co−C bond cleavage and hydrogen-transfer events.[46,47] The composite bond cleavage/hydrogen-transfer step corresponds to a direct $A_1 \rightarrow A_3$ transition in Scheme 1, and we use the subscript

dx.doi.org/10.1021/ja404467d | J. Am. Chem. Soc. 2013, 135, 15077−15084

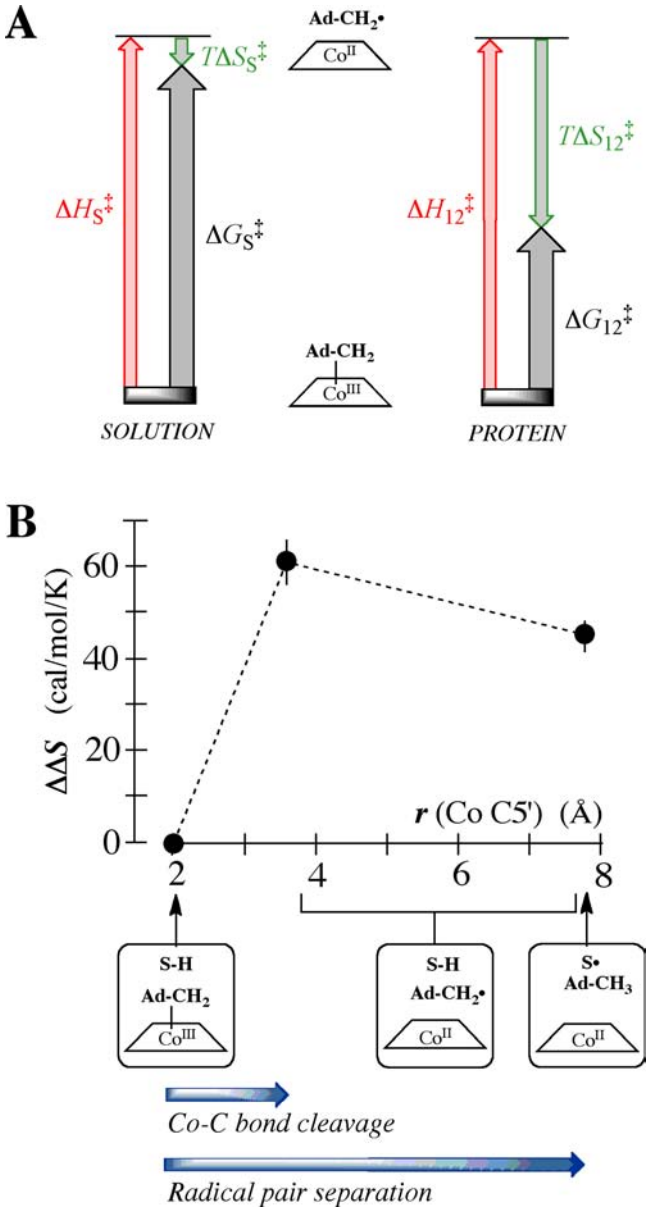

Figure 5. Representations of the activation parameters for Co−C bond cleavage in solution and in the EAL protein, and entropy contributions during radical pair separation in EAL. (A) Activation parameters for Co−C cleavage in solution[45] and in EAL (this work). The values of $T\Delta S^{\ddagger}$ correspond to T = 298 K. The free energy levels of the initial AdoCbl states in solution and in EAL are aligned, for illustration. (B) Activation entropy change for Co−C bond cleavage, and the equilibrium entropy change for formation of the Co(II)−substrate radical pair,[25] both referenced to the EAL ternary complex. The Co−C5′ separation distances at the transition state for bond cleavage and in the Co(II)−substrate radical pair state are estimated from calculations[11] and determined by using pulsed-EPR spectroscopy,[63] respectively. The positions of the ternary complex, Co(II)−5′-deoxyadenosyl radical pair, and Co(II)−substrate radical pair on the Co−C5′ separation coordinate are indicated.

"13" to denote this in the following. For the dGTP activator-initiated Co−C bond cleavage to form the intermediate Co(II)−cysteine thiyl radical pair in RTPR in the absence of bound substrate, the observed activation parameters are $\Delta H^{\ddagger}_{13}$ = 46 ± 7 kcal/mol and $\Delta S^{\ddagger}_{13}$ = 96 ± 12 cal/(mol·K) ($T\Delta S^{\ddagger}_{13}$ = 29 ± 4 kcal/mol at 298 K).[46] Licht et al.[46] concluded that favorable entropic factors make the largest contribution to catalysis of Co(II)−thiyl radical pair formation in RTPR, and they speculated that release of bound water (hydrophobic effect) or an increase in protein conformational flexibility were the most likely molecular mechanisms. In contrast, in MCM, $\Delta H^{\ddagger}_{13}$ = 18.8 ± 0.8 kcal/mol and $\Delta S^{\ddagger}_{13}$ = 18.2 ± 0.8 cal/(mol·K) ($T\Delta S^{\ddagger}_{13}$ = 5.3 ± 0.2 kcal/mol at 298 K), and it was concluded that enthalpic factors were dominant in the catalysis of Co(II)−substrate radical pair formation.[47] Although the activation parameters for RTPR and MCM include contributions from both the Co−C bond cleavage and hydrogen-transfer steps, the results suggest that favorable activation entropy changes also contribute significantly to Co−C bond cleavage in other AdoCbl-dependent enzymes.

Proposed Protein Configurational Entropy Contribution to Co−C Bond Cleavage Catalysis in EAL. We propose a "configurational catalysis" model, which accounts for the relation $\Delta S^{\ddagger}_{12} \gg \Delta S^{\ddagger}_{S}$, in which protein configurational entropy increases along the Co−C bond cleavage coordinate. The total configurational entropy, S_{conf}, of the protein can be written as follows:[48]

$$S_{conf} = \sum_{i=1}^{N} p_i S_i^{I} - k_B \sum_{i=1}^{N} p_i \ln p_i \qquad (6)$$

The first term on the right-hand side of eq 6 represents an individual protein configuration, i, with Boltzmann weighting factor p_i and entropy S_i^{I}, and the second term represents the number of distinct protein configurations. The difference between S_{conf} at the transition state and at the equilibrium reactant state contributes to $\Delta S^{\ddagger}_{12}$. The reduced-dimension free energy landscape in Figure 6A illustrates the model. In the free energy landscape depiction, an increase of S_i^{I} deepens the channel along a particular reaction path. Increases in S_i^{I} could arise from conversion of a subset of harmonic modes to lower frequency,[49] although enthalpy−entropy compensation[50] appears to limit significant contributions from this term. Therefore, the dominant contribution of S_{conf} to the activation entropy for Co−C bond cleavage is proposed to arise from the configurational entropy term in eq 6. The increase of the configurational entropy with progress along the reaction coordinate is represented as a ramification of paths in Figure 6A, which leads to the relatively broad saddle region at the transition state. Figure 6B illustrates the contrasting case for a reaction with no configurational entropy change. The microscopic origin of the activation entropy involves relatively small protein configurational changes, because these satisfy the constraint that the configurations are approximately isoenergetic (relative to the transition state barrier height), as indicated by the monotonic reaction kinetics. Specific, localized intereactions of cofactor and protein, such as those of the type described in detailed mechanistic proposals,[17−20] would couple changes in cofactor structure and protein configurational states.

The favorable contributions of multiple paths through configuration space to the free energy barriers of chemical reactions in solution[51] and in enzymes[52] have been considered. The model for configurational entropy-promoted enzyme catalysis, or "configurational catalysis", that is illustrated in Figure 6A, is supported by experimental studies that show significant configurational entropy contributions to other protein processes. Nuclear magnetic resonance relaxation measurements show a substantial "residual" entropy in folded

dx.doi.org/10.1021/ja404467d | J. Am. Chem. Soc. 2013, 135, 15077−15084

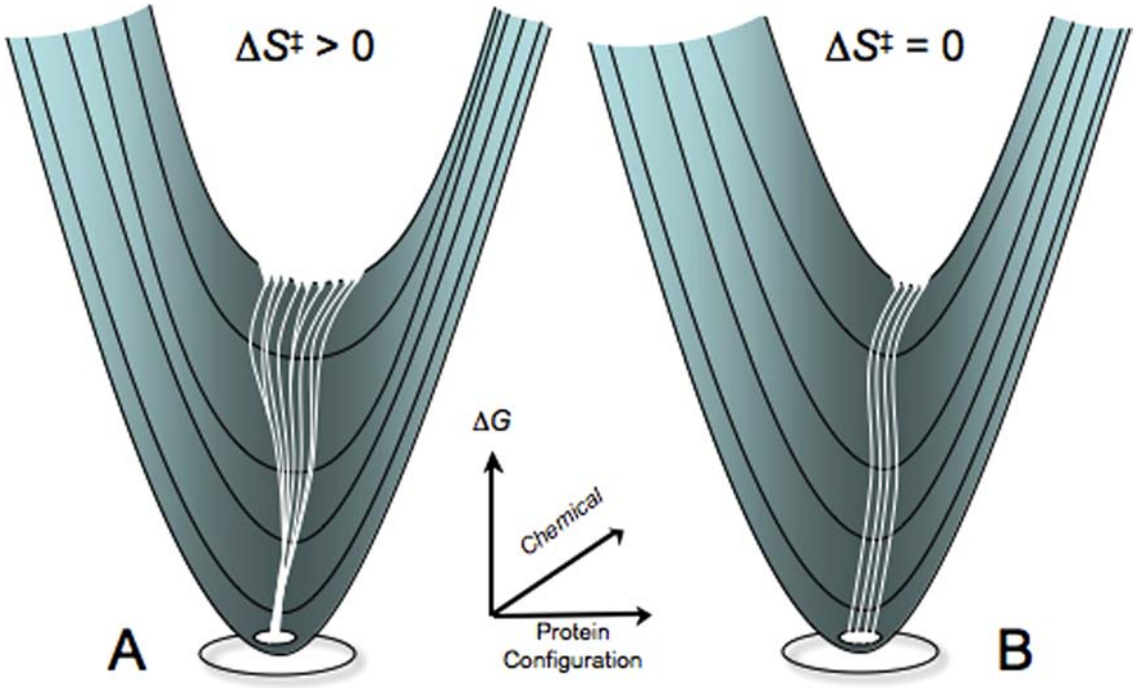

Figure 6. Free energy landscape representations of the chemical coordinate for Co−C bond cleavage and reduced protein configurational coordinates. (A) Model proposed to account for activation entropy in EAL for the Co−C bond cleavage reaction. Progress along the reaction coordinate is associated with the creation of new configurations and a relatively broad saddle point region. The width of the saddle point represents the relative configurational entropy contribution to the activation free energy. (B) Representation of a reaction with no configurational entropy contribution to the activation entropy. The number of configurations does not change between reactant and transition states.

proteins[53] and that protein entropy contributions to equilibrium ligand-protein binding arise from both terms in eq 6.[54−56] The "folding funnel" description of favorable configurational contributions to protein denaturation[57] bears similarity to the model, although the protein configurations depicted in Figure 6A all lie within the manifold of globally folded states. The configurational catalysis model is consistent with the low quantum yield ($<10^{-2}$) of Co(II)−radical pair formation observed in transient photolysis studies of AdoCbl in the EAL ternary complex at 240 K,[16] changes in EAL protein secondary structure following Co−C bond thermolysis detected by infrared spectroscopy,[58] and the solution viscosity dependence of the Co(II)−radical pair lifetime in EAL.[59]

■ CONCLUSION

The temperature dependence and hydrogen isotope independence of the first-order kinetics of Co(II)−substrate radical pair formation from the ternary complex in EAL in a low-temperature cryosolvent system show that Co−C bond cleavage catalysis of AdoCbl in EAL, relative to that in solution, arises from a large, favorable activation entropy, $\Delta S^{\ddagger}_{12} = 61 \pm 6$ cal/(mol·K). Co−C bond cleavage does not solely rate-determine radical pair formation at ambient temperatures, because the term $-T\Delta S^{\ddagger}_{12}$ decreases the activation free energy, $\Delta G^{\ddagger}_{12}$, as the temperature is raised. This causes emergence of rate determinaton by the hydrogen-transfer step that follows Co−C bond cleavage, consistent with the $^{1}H/^{2}H$ isotope effect of 3.1 on Co(II)−substrate radical pair formation in EAL at ambient temperature.[10,30] The entropic origin of Co−C bond cleavage catalysis in EAL represents a paradigm shift from traditional, enthalpy-based proposals.[5,14,17,18] We propose a model of "configurational catalysis", in which ramification of protein configurations along the reaction coordinate leads to the favorable activation entropy. This model has parallels in the significant protein configurational entropy changes associated with protein−ligand interactions[53−55] and protein unfolding[57] and is consistent with transient kinetic and spectroscopic studies of EAL.[16,58,59] The results provide the perspective that acceleration of individual steps in multistep enzyme reaction sequences by entropic contributions, such as those described here, is more prevalent than previously recognized. Low (cryogenic) temperatures are required to decrease the value of $T\Delta S^{\ddagger}$, and thus increase $\Delta G^{\ddagger}$, to expose entropically catalyzed steps. However, the dual stringent requirements of maintenance and measurement of enzyme function at low temperatures are not met, commonly. Understanding the microscopic origins of the activation entropy contribution to Co−C bond cleavage in EAL, and in other enzymes, may illuminate "missing" components of enzyme catalysis[60] and propel an "entropy engineering" approach to rational design of protein catalysts, to parallel the traditional focus on control through manipulation of interaction energy (enthalpy).

■ ASSOCIATED CONTENT

Supporting Information

X-band continuous-wave EPR spectra of the Co(II)−substrate radical pair formed from ^{2}H and ^{1}H substrate at low temperature in DMSO/water cryosolvent; Arrhenius plots of the observed first-order rate constant for formation of the Co(II)−substrate radical pair as a function of inverse absolute temperature for ^{2}H and ^{1}H substrates; composite Arrhenius plot of the observed first-order rate constant for formation of the Co(II)−substrate radical pair as a function of inverse absolute temperature for ^{2}H and ^{1}H substrates; table of values of the rate constant for Co−C bond cleavage for ^{2}H and ^{1}H

dx.doi.org/10.1021/ja404467d | J. Am. Chem. Soc. 2013, 135, 15077−15084

substrates at different temperatures. This material is available free of charge via the Internet at http://pubs.acs.org.

AUTHOR INFORMATION

Corresponding Author

kwarncke@physics.emory.edu

Present Address

‡M.W.: Wilmad-LabGlass, 1172 NW Blvd., Vineland, NJ 08360

Notes

The authors declare no competing financial interest.

ACKNOWLEDGMENTS

We thank Dr. Li Sun, Dr. Adonis M. Bovell, and Prof. Vincent Huynh for helpful discussions. Research reported in this publication was supported by the National Institute of Diabetes and Digestive and Kidney Diseases of the National Institutes of Health under Award Number R01 DK054514. The purchase of the Bruker E500 EPR spectrometer was funded by the National Center for Research Resources of the National Institutes of Health under Award Number RR17767, and by Emory University.

REFERENCES

(1) Banerjee, R. *Chemistry and Biochemistry of B12*; Wiley: New York, 1999.
(2) Brown, K. L. *Chem. Rev.* **2005**, *105*, 2075.
(3) Frey, P. A. In *Comprehensive Natural Products II Chemistry and Biology*; Mander, L., Lui, H.-W., Eds.; Elsevier: Oxford, 2010; Vol. 7, p 501.
(4) Hay, B. P.; Finke, R. G. *Polyhedron* **1988**, *7*, 1469.
(5) Brown, K. L. *Dalton Trans.* **2006**, 1123.
(6) Padmakumar, R.; Padmakumar, R.; Banerjee, R. *Biochemistry* **1997**, *36*, 3713.
(7) Marsh, E. N. G.; Ballou, D. P. *Biochemistry* **1998**, *37*, 11864.
(8) Cheng, M.-C.; Marsh, E. N. G. *Biochemistry* **2007**, *46*, 883.
(9) Licht, S. S.; Booker, S.; Stubbe, J. *Biochemistry* **1999**, *38*, 1221.
(10) Bandarian, V.; Reed, G. H. *Biochemistry* **2000**, *39*, 12069.
(11) Kozlowski, P. M.; Kamachi, T.; Toraya, T.; Yoshizawa, K. *Angew. Chem.* **2006**, *119*, 998.
(12) Pang, J.; Li, X.; Morokuma, K.; Scrutton, N. S.; Sutcliffe, M. J. *J. Am. Chem. Soc.* **2012**, *134*, 2367.
(13) Shibata, N.; Tamagaki, H.; Hieda, N.; Akita, K.; Komori, H.; Shomura, Y.; Terawaki, S.; Mori, K.; Yasuoka, N.; Higuchi, Y.; Toraya, T. *J. Biol. Chem.* **2010**, *285*, 26484.
(14) Garr, C. D.; Sirovatka, J. M.; Finke, R. G. *Inorg. Chem.* **1996**, *35*, 5912.
(15) Robertson, W. D.; Warncke, K. *Biochemistry* **2009**, *48*, 140.
(16) Robertson, W. D.; Wang, M.; Warncke, K. *J. Am. Chem. Soc.* **2011**, *133*, 6968.
(17) Sharma, P. K.; Chu, Z. T.; Olsson, M. H. M.; Warshel, A. *Proc. Natl. Acad. Sci. U.S.A.* **2007**, *104*, 9661.
(18) Toraya, T. *Chem. Rev.* **2003**, *103*, 2095.
(19) Bucher, D.; Sandala, G. M.; Durbeej, B.; Radom, L.; Smith, D. M. *J. Am. Chem. Soc.* **2012**, *134*, 1591.
(20) Kwiecien, R. A.; Khavrutskii, I. V.; Musaev, D. G.; Morokuma, K.; Banerjee, R.; Paneth, P. *J. Am. Chem. Soc.* **2006**, *128*, 1287.
(21) Brooks, A. J.; Vlasie, M.; Banerjee, R.; Brunold, T. C. *J. Am. Chem. Soc.* **2004**, *126*, 8167.
(22) Brooks, A. J.; Vlasie, M.; Banerjee, R.; Brunold, T. C. *J. Am. Chem. Soc.* **2005**, *127*, 16522.
(23) Dong, S. L.; Padmakumar, R.; Banerjee, R.; Spiro, T. G. *J. Am. Chem. Soc.* **2004**, *121*, 7063.
(24) Sension, R. J.; Harris, A. D.; Stickrath, A.; Cole, A. G.; Fox, C. C.; Marsh, E. N. G. *J. Phys. Chem. B* **2005**, *109*, 18146.
(25) Wang, M.; Warncke, K. *J. Am. Chem. Soc.* **2008**, *130*, 4846.
(26) Hubbard, T. J. P.; Ailey, B.; Brenner, S. E.; Murzin, A. G.; Chothia, C. *Nucleic Acids Res.* **1999**, *27*, 254.
(27) Sun, L.; Warncke, K. *Proteins* **2006**, *64*, 308.
(28) Bovell, A. M.; Warncke, K. *Biochemistry* **2013**, *52*, 1419.
(29) Bradbeer, C. *J. Biol. Chem.* **1965**, *240*, 4669.
(30) Bandarian, V.; Reed, G. H. In *Chemistry and Biochemistry of B12*; Banerjee, R., Ed.; John Wiley and Sons: New York, 1999; p 811.
(31) Faust, L. R. P.; Connor, J. A.; Roof, D. M.; Hoch, J. A.; Babior, B. M. *J. Biol. Chem.* **1990**, *265*, 12462.
(32) Faust, L. P.; Babior, B. M. *Arch. Biochem. Biophys.* **1992**, *294*, 50.
(33) Wang, M. Ph.D. Dissertation, Emory University, 2009.
(34) Hollaway, M. R.; White, H. A.; Joblin, K. N.; Johnson, A. W.; Lappert, M. F.; Wallis, O. C. *Eur. J. Biochem.* **1978**, *82*, 143.
(35) Moore, J. W.; Pearson, R. G. *Kinetics and Mechanism*; Wiley and Sons: New York, 1981.
(36) Bevington, P. R.; Robinson, D. K. *Data reduction and error analysis for the physical sciences*, 2nd ed.; WCB/McGraw-Hill: St. Louis, 1992.
(37) Babior, B. M.; Moss, T. H.; Orme-Johnson, W. H.; Beinert, H. *J. Biol. Chem.* **1974**, *249*, 4537.
(38) Cleland, W. W. *Crit. Rev. Biochem. Mol.* **1982**, *13*, 385.
(39) McMillen, D. F.; Golden, D. M. *Annu. Rev. Phys. Chem.* **1982**, *33*, 493.
(40) Berkowitz, J.; Ellison, G. B.; Gutman, D. *J. Phys. Chem.* **1994**, *98*, 2744.
(41) Wetmore, S. D.; Smith, D. M.; Bennet, J. T.; Radom, L. *J. Am. Chem. Soc.* **2002**, *124*, 14054.
(42) Sandala, G. M.; Smith, D. M.; Radom, L. *J. Am. Chem. Soc.* **2005**, *127*, 8856.
(43) Cheng, M.-C.; Marsh, E. N. G. *Biochemistry* **2005**, *44*, 2686.
(44) Chen, D.; Abend, A.; Stubbe, J.; Frey, P. A. *Biochemistry* **2003**, *42*, 4578.
(45) Hay, B. P.; Finke, R. G. *J. Am. Chem. Soc.* **1986**, *108*, 4820.
(46) Licht, S.; Lawrence, C. C.; Stubbe, J. *Biochemistry* **1999**, *38*, 1234.
(47) Chowdhury, S.; Banerjee, R. *Biochemistry* **2000**, *39*, 7998.
(48) Karplus, M.; Ichiye, T.; Pettitt, B. M. *Biophys. J.* **1987**, *52*, 1083.
(49) Sturtevant, J. M. *Proc. Natl. Acad. Sci. U.S.A.* **1977**, *74*, 2236.
(50) Lumry, R.; Rajender, S. *Biopolymers* **1970**, *9*, 1125.
(51) Leffler, J. E.; Grunvald, E. *Rates and equilibria of organic reactions*; Dover: New York, 1989.
(52) Kamerlin, S. C. L.; Warshel, A. *Proteins* **2011**, *78*, 1339.
(53) Li, Z.; Raychaudhuri, S.; Wand, A. J. *Protein Sci.* **1996**, *5*, 2647.
(54) Igumenova, T. I.; Frederick, K. K.; Wand, A. J. *Chem. Rev.* **2006**, *106*, 1672.
(55) Frederick, K. K.; Marlow, M. S.; Valentine, K. G.; Wand, A. J. *Nature* **2007**, *448*, 325.
(56) Wand, A. J. *Curr. Opin. Struct. Biol.* **2013**, *23*, 75.
(57) Onuchic, J. N.; Wolynes, P. G. *Curr. Opin. Struct. Biol.* **2004**, *14*, 70.
(58) Russel, H. J.; Jones, A. R.; Hay, S.; Greetham, G. M.; Towrie, M.; Scrutton, N. S. *Angew. Chem., Int. Ed.* **2012**, *51*, 9306.
(59) Jones, A. R.; Hardman, S. J. O.; Hay, S.; Scrutton, N. S. *Angew. Chem.* **2011**, *123*, 11035.
(60) Kraut, D. A.; Carrol, K. S.; Herschlag, D. *Annu. Rev. Biochem.* **2003**, *75*, 517.
(61) Ke, S.-C.; Torrent, M.; Museav, D. G.; Morokuma, K.; Warncke, K. *Biochemistry* **1999**, *38*, 12681.
(62) Abend, A.; Bandarian, V.; Nitsche, R.; Stupperich, E.; Retey, J.; Reed, G. H. *Arch. Biochem. Biophys.* **1999**, *370*, 138.
(63) Canfield, J. M.; Warncke, K. *J. Phys. Chem. B* **2002**, *106*, 8831.